Using Electrical Resistivity Methods and Traditional Survey Techniques to Delineate Potential Karst Features Along FM 2185, Culberson County, Texas

By Lenora Perkins

Department of Geology

Excerpt from Master's Thesis

Using Electrical Resistivity Methods and Traditional Survey Techniques to Delineate Potential Karst Features Along FM 2185, Culberson County, Texas

Abstract

The Delaware Basin of West Texas and New Mexico is the major western subdivision of the Permian Basin. The study area, located within Culberson County, Texas, traverses a distance of 30-miles (48 km) along Farm to Market Road 2185 (FM 2185) within the Gypsum Plain. This area includes outcrops of the Castile Formation, which is host to karst geohazards such as sinkholes, subsidence features, and caves from the dissolution of evaporite strata. The extensive karst development in this region poses a significant geohazard threat to infrastructure. Land reconnaissance surveys conducted during summer of 2019 documented numerous surficial manifestations of karst features proximal to FM 2185.

In combination with traditional survey techniques, electrical resistivity methods were used to delineate karst features that pose potential geohazard concerns along the 30-mile (48 km) segment of FM 2185. Data was acquired with the Geometrics OhmMapper G-858 TR5 resistivity system, which uses a dipole-dipole configuration composed of five receivers connected by 2.5-meter coaxial cables and a 5-meter non-conductive rope. This geometric configuration enabled resistivity readings up to ~2.5 meters deep. Data was processed using AGI's (Advanced Geometrics Inc.) EarthImager 2D software and used to delineate karst related cavities and voids for improved roadway design.

INTRODUCTION

The Delaware Basin of West Texas and southeast New Mexico hosts widespread karst development throughout the Gypsum Plain, which covers an area of ~ 2800 km^2 (Hill, 1996). The evaporite outcrops found within this area include Permian-aged Castile and Rustler formations. Features commonly expressed in this region are comprised of a wide array of

surficial karst manifestations, as well as shallow epigene caves, and deeper, more complex hypogene cave systems (Stafford et al., 2008a, 2008b). Evaporite karst systems can be complex and rapidly evolve due to higher solution rates than carbonates. Depending on hydrogeologic conditions, dissolution of evaporite karst can occur within days, weeks, or years while in carbonate karst, the rates of void enlargement rarely achieve significance within the human lifetime (Klimchouk and Askem, 2005).

Oil exploration in the Permian Basin has a long and rich history since the 1920s. As of January 2020, the Permian Basin has produced more than 35.6 billion barrels of oil and ~125 trillion cubic feet of natural gas (EIA, 2020). Within the last decade there have been advances in the Delaware Basin targeting unconventional reservoirs such as the Bone Spring Formation and the Delaware Mountain Group (EIA, 2020). The intensification in hydrocarbon extraction and exploration has led to an increase in development of vehicle infrastructure along with an associated rise of incidents related to karst geohazards. According to Stafford et al. (2017), the existing roads in this area were not initially designed to accommodate the heavy volume, and weight, of oilfield traffic and therefore are subject to collapse.

Traditional survey techniques such as field mapping may be used to identify karst hazards that manifest at the land surface in areas with absent or patchy cover sediments (Neukum et al., 2010). However, karst features that do not manifest surficially require alternative surveying methods to characterize the extent of subsurface features at depth. Over the past decade, various methods have been implemented to characterize occurrence of Gypsum Plain karst, and due to the expansion of oilfield activity into the region, remote sensing, and GIS (Geographic Information System) techniques have been used more frequently (Woodard, 2017; Majzoub et al., 2017; Stafford 2008b, Stafford et al., 2017; Land et al., 2018). Studies conducted by Woodard (2017) and Stafford et al. (2017) demonstrate that Capacitively-Coupled Resistivity (CCR) surveys are effective in the detection of shallow subsurface karst features.

The study presented here was conducted along 30-mile (48 km) segment of undeveloped Farm to Market Road 2185 (FM 2185) in Culberson County, Texas Figure 1. The dissolution of evaporite strata of the Castile and Rustler formations have led to the formation of numerous karst geohazard phenomena including sinkholes, subsidence features, and caves. Land reconnaissance surveys conducted during summer of 2019 documented numerous surficial manifestations of

karst features proximal to FM 2185. This study effectively utilizes CCR methods to characterize and delineate concealed karst features that could lead to potential geohazard concerns. Two survey sites are presented in this study as examples of the effectiveness of the CCR imaging in the rapid delineation of potential geohazards.

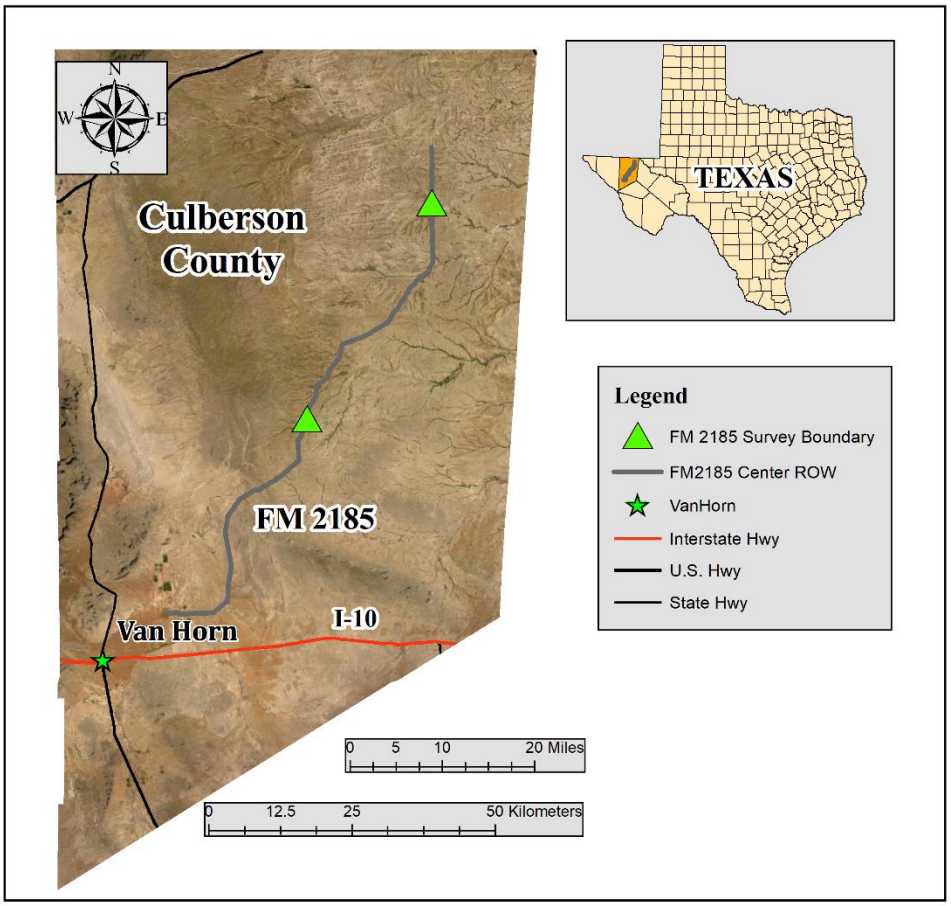

Figure 1: *Geographic location of the study area, FM 2185 in thickened gray line stretching southwest to northeast across Culberson County, Texas. Survey boundary indicated by green triangles.*

GEOLOGIC SETTING

The Delaware Basin of West Texas and southeastern New Mexico is an irregular, inverted pear-shaped intracratonic depositional basin, Figure 2. As the major western subdivision of the Permian Basin, it encompasses an area of 33,500 km^2 with a length of 250 km and width of 180 km that is restricted by the Capitan Reef Complex (Hill, 1996). From the late Precambrian to the Late Mississippian, the Delaware Basin was part of the Tobosa Basin. During that time,

shelf sediments accumulated in a “layer-cake” fashion due to passive subsidence, as well as the warping and sagging of the Tobosa Basin (Horak, 1985b).

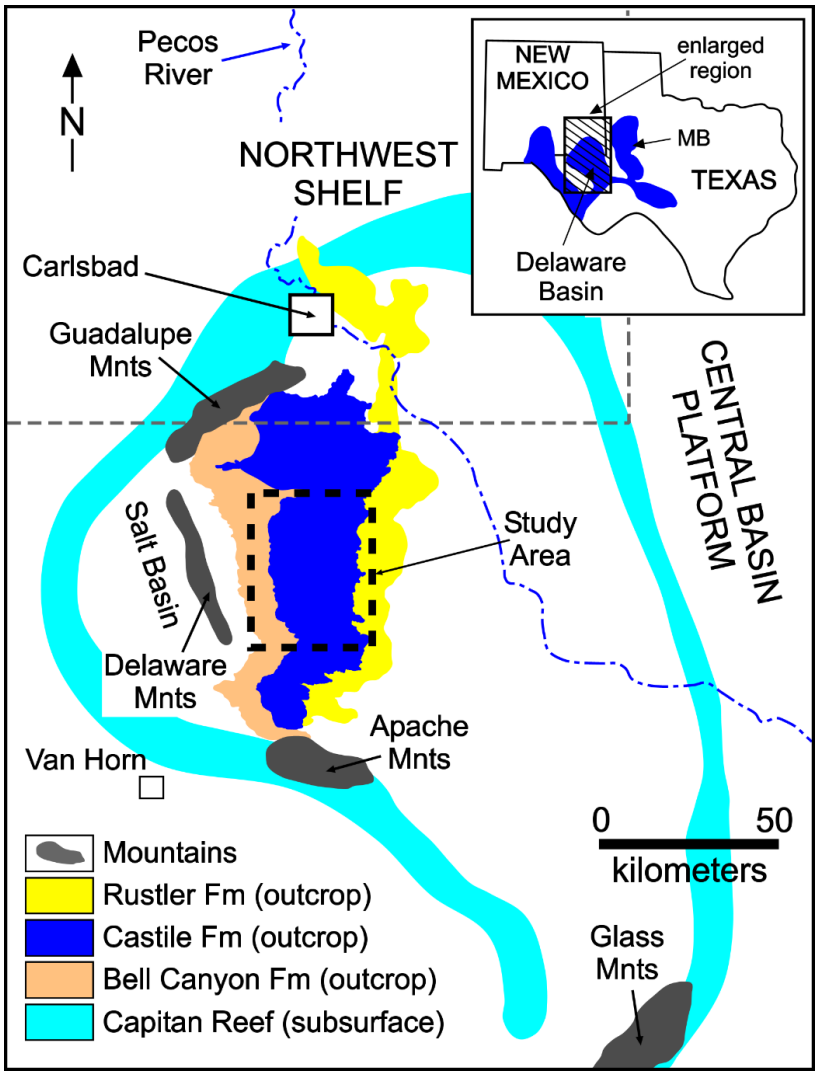

Figure 2: *Map illustrating the geographic orientation of the Delaware Basin in West Texas and southeastern New Mexico. The primary geologic features of the region are outlined. The study area is outlined by the dashed black line. MB = Midland Basin.*

During the Late Mississippian through Early Permian (310-265 Ma), a major tectonic episode occurred in the area of the Delaware Basin. Initiated by the formation of Pangea, mild tectonic activity accompanied vertical movement along zones of weakness from late Precambrian lateral faulting (Keller et al., 1980). This tectonic episode produced the Ouachita orogeny in the Marathon-Delaware Basin area. Additionally, uplift of the Central Basin Platform induced the division of the Tobosa Basin into three segments: the uplifted Central Basin

Platform, and the down-dropped Delaware and Midland basins (Hill, 1996). Broad limestone shelves grew to surround these three smaller basins as they formed. Stream channels eventually cut through the limestone shelves to deposit fine sands and shales into the basins (Keller et al., 1980). In the Pennsylvanian, increased compression from the Ouachita orogenic front led to the rapid subsidence of the Delaware Basin, where it remained a deep-water basin until the end of the Guadalupian time (Hill, 1996).

Extensive reef growth occurred during the Ochoan, which restricted the flow of open marine waters and incited the formation of a deep saline lake that possessed conditions conducive for the deposition of Castile evaporites. Although the Castile deposition was limited to the Delaware Basin, the deposition of Salado and Rustler strata capped the region and surrounding basins (Scholle et al., 2004). The tectonic activity that occurred during the Early Mesozoic had little effect on the Delaware Basin; however, the Laramide Orogeny of the Late Mesozoic and Early Cenozoic produced regional tilting and uplift of the basin strata 3-5° to the east-northeast.

Following Laramide deformation, the Basin and Range phase consisted of lithospheric thinning, extension, and normal faulting. Volcanism also ensued during this time to produce a regime of higher heat flow in the Delaware Basin with geothermal gradients reaching 40-50° C/km or more (Barker and Pawliewicz, 1987). The hydrothermal regime shifted from one of melting and igneous intrusions to one of an increased temperature gradient and convective heat flow. During the Oligocene, hydrothermal cells were formed by igneous intrusions which allowed deeply circulating fluids to move along fault zones and paleokarst systems. This circulating hydrothermal water could have then alternately dissolved limestone in the solutional zone and precipitated calcite in the depositional zone.

During the Quaternary, both the effects of Basin and Range extension and the geothermal gradient decreased. The present-day geothermal gradient in the Delaware Basin is roughly 20°C/km as compared to the Miocene paleogradient of 40-50°C/km (Barker and Halley, 1986; Barker and Pawliewicz, 1993). Additionally, during the Pleistocene the Delaware Basin experienced considerable fluctuations in climate from wet and cold to dry and warm during glacial and interglacial periods. The modern landscape of the Gypsum Plain was sculpted through intermittent periods of heavy stream erosion during glacial melt and karst processes.

Over the last 10,000 years, the changes in climate allowed the Delaware Basin to transition from a cool and wet climate to one that is dry and arid-semiarid.

KARST DEVELOPMENT

The Permian evaporites of the Gypsum Plain have resulted in a quickly evolving landscape throughout the Delaware Basin. The Castile Formation is the largest continuous outcrop of evaporites in the area and represent deep-water deposits, which are subsequently covered by the Salado and Rustler formations. Minor occurrences of karst development are noted in the evaporites of lower Rustler strata located on the eastern portion of the study area. The halite-rich Salado Formation is almost completely dissolved from outcrop and shallow subcrop via intrastratal dissolution, thus forming an irregular solutional contact boundary between the Castile and Rustler strata (Stafford et al., 2008a). The lower bounding horizon is the siliciclastic Bell Canyon Formation, which provides ascending fluids for hypogene speleogenesis (Stafford et al., 2018). Models of the current and paleo hydrogeologic system of the Delaware Basin, derived by Lee and Williams (2000), indicate that the Bell Canyon aquifer is mixing ascending fluids and hydrocarbons from deep basinal units.

In the Delaware Basin, the Castile Formation hosts extensive cave and karst development across 1800 km^2 of outcrop. Surficial karren dominate the landscape with abundant sinkholes, subsidence features, and solution-widened fractures. Epigene and hypogene speleogenesis both account for the formation of solutional caves in this region. Epigene caves develop from gravitationally driven water from near-surface meteoric processes in unconfined strata, while hypogene caves manifest via dissolution from rising fluids from the underlying Bell Canyon Formation driven by differences in hydraulic pressure gradients through semi-confined strata (Stafford et al, 2008a).

Also present within the study area are gypsite suffosion caves, or gypsite soil caves, and collapsed breccia pipes. In the study area, suffosion caves commonly develop from the preferential transport of gypsic soils through thick soil horizons and soil-filled solutional sinkholes (Stafford et al, 2017). Zones of brecciation extending laterally and vertically hundreds

of meters that formed as the result of intrastratal dissolution of evaporites at depth through hypogene speleogenesis that subsequently stoped upwards (Stafford et al, 2008a).

ELECTRICAL RESISTIVITY METHODS

A continuous, CCR survey was conducted along a 30-mile segment of the proposed route of FM 2185 in Culberson County, Texas Figure1. The CCR data was acquired with the Geometrics OhmMapper G-858 resistivity system that uses a dipole-dipole TR-5 configuration composed of five receivers and one transmitter connected by 2.5-meter coaxial cables, with a transmitter offset of 2.5 meters. The OhmMapper G-858 resistivity meter was attached to a vehicle and towed at a steady pace, Figure 3. Data was collected at a transmission rate of once per second and traverse speed of ~2.5-3 km/h. A Trimble Nomad 900 series logger, a Global Positioning System (GPS) unit, connected to a Pathfinder Pro receiver and Zephyr antennae recorded the traversed survey with a horizontal accuracy of less than 50 cm.

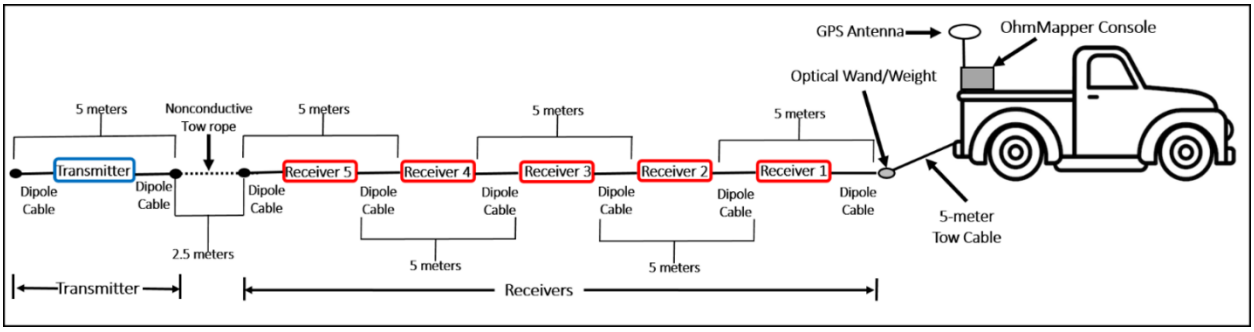

***Figure 3**: Diagram of OhmMapper TR-5 resistivity meter configuration. Diagram illustrates a CCR TR-5 configuration with five receivers and one transmitter. This allowed for five discrete depth resistivity measurements while continuously collecting data along the traverse.*

Prior to inversion, the quality of the CCR data and GPS points gathered with the OhmMapper G-858 resistivity meter were preprocessed using MagMap2000, a pre-inversion software program developed by Geometrics. For all collected resistivity data, inversion was performed in AGI's *EarthImager 2D* inverse modelling software. To accurately represent the elevation variance at each site, terrain corrections were applied. Elevation values were extracted from a digital elevation model created from LiDAR (Light Detection and Ranging) data of the

study area and processed in ArcGIS. LiDAR horizontal resolution was acquired at 0.3-0.4 meters with 10 centimeters vertical resolution (Ehrhart, 2016).

SITE ANALYSIS & INTERPRETATIONS

Site 1 (120-m Survey)

Site 1, located within the Castile Formation, Figure 4, contains shallow gypsic soil, 0.5-1.0m depth, overlying a non-uniformly cemented breccia pipe that has been largely calcitized through sulfate reduction associated with hypogene processes. The land surface exhibits elevation difference of 1m, moderate vegetation, and proximal surface exposures of indurated gypsic soil, poorly-cemented brecciated gypsum, and cemented calcitized breccia. Data presented is a 120m segment of CCR data extracted from ~1km of continuous CCR survey of an undeveloped segment of FM 2185. Successful depth of investigation is ~2.5m.

The resistivity image presented in Figure 5 displays a portion of the breccia pipe that extends from meter mark 0-95 and 105-115 along the resistivity profile, which is likely connected at depths greater than CCR investigation. High resistivity signature within the breccia pipe at meter mark 47 is interpreted as probable fracturing and high moisture flux. Within the breccia pipe, well-cemented brecciated gypsum and porous, poorly-cemented, calcitized areas are discernable, likely as a result of variable moisture content within variably porous media.

Site 2 (120-m Survey)

Site 2 is located in an area of the Castile Formation significantly mantled and infilled with gypsic soil, Figure 6. The region is noted by an elevation difference of 0.5m and an area of dense vegetation. Data presented is a 120m segment of CCR data extracted from ~1km of continuous CCR survey of an undeveloped segment of FM 2185, Figure 7. Successful depth of investigation is to 2.5m.

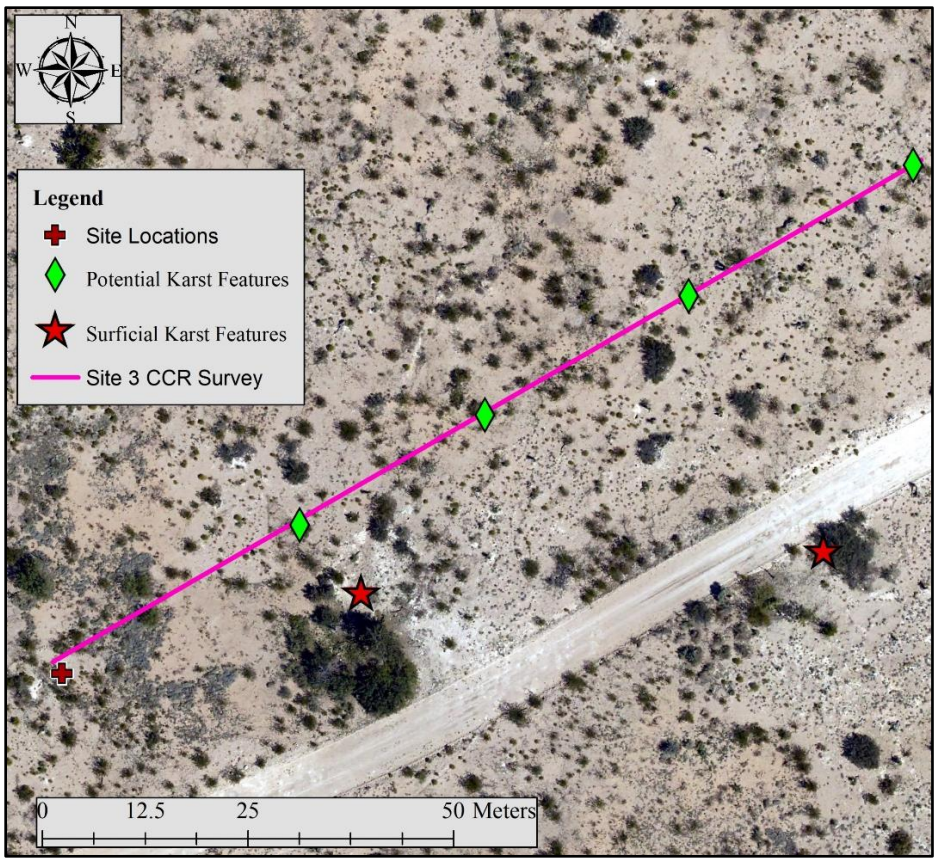

Figure 4: *Orthoimagery image of Site 1. Green diamonds represent potential karst features detected from CCR data, red stars indicate mapped surficial karst features, the pink line is the CCR survey line.*

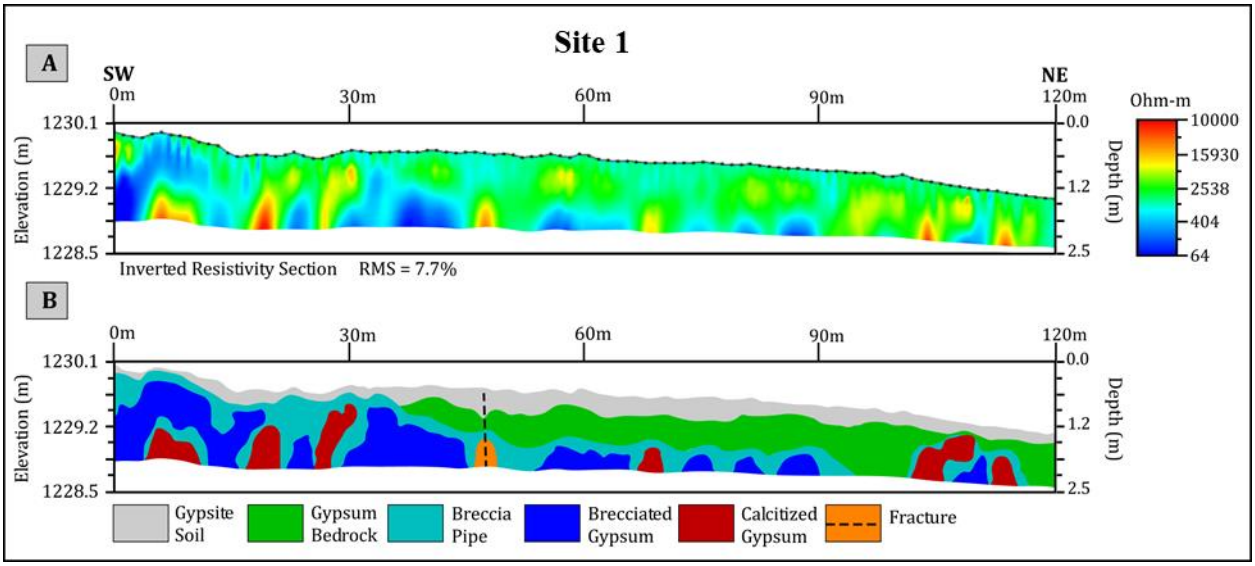

Figure 5: *Site 1, 120m segment of CCR data. A) inverted resistivity section to a depth of ~2.5m, RMS = 7.7%; B) interpreted inverted section. Depth of investigation is ~2.5m.*

This site is proximal to mapped surficial karst features (Figure 6) and numerous anomalous patterns were modeled within the resistivity inversions. Within the CCR data, from meter mark 5-45, and 0.5-2.5m in depth, is a zone of extensively collapsed gypsite. At meter mark 35 and 65, and 2.0m deep, a high resistivity anomaly is interpreted as a probable, un-collapsed gypsite cave.

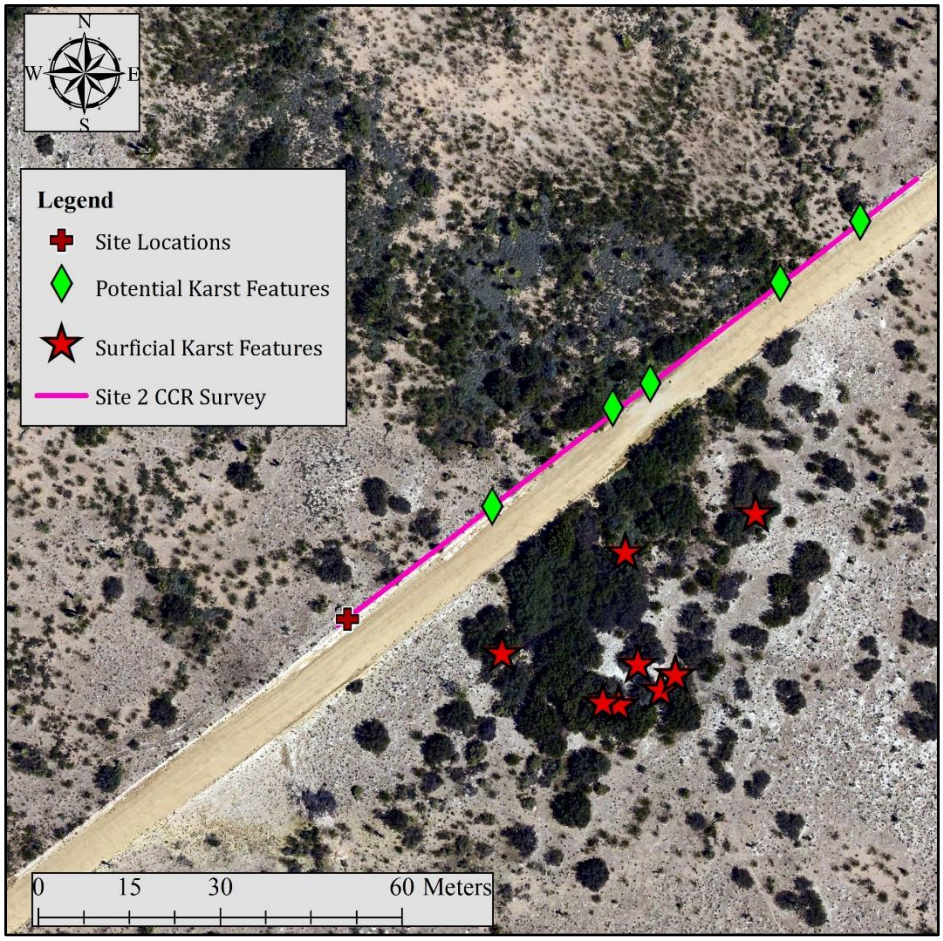

Figure 6: *Orthoimagery of Site 5. Green diamonds represent potential karst features detected from CCR data, red stars indicate mapped surficial karst features, the pink line is the CCR survey line.*

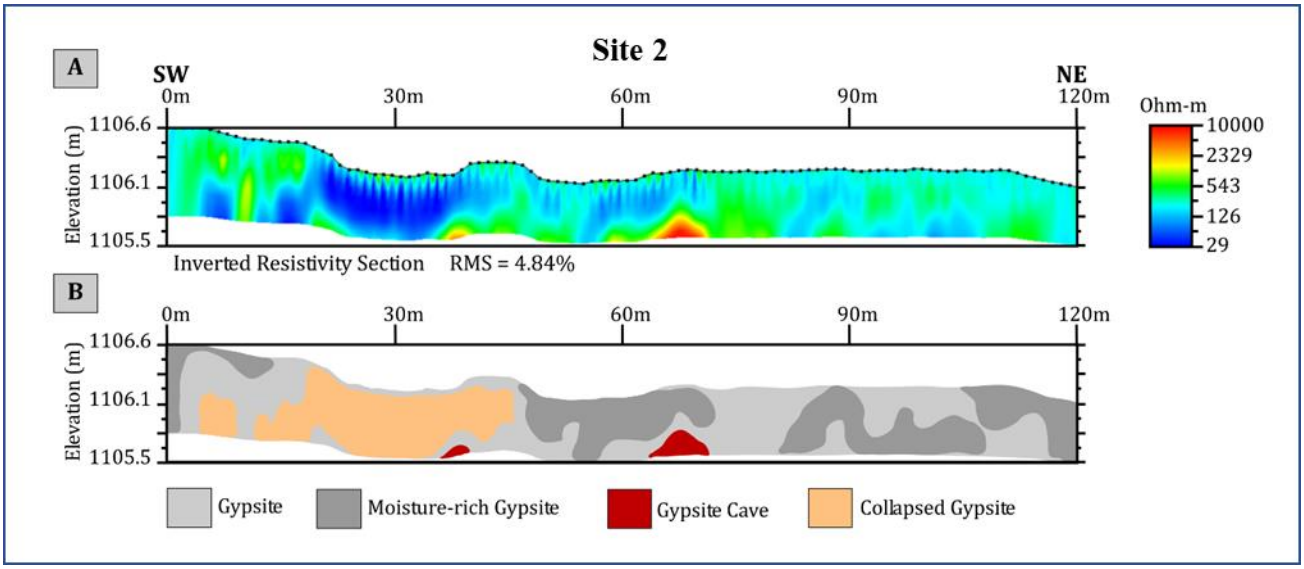

Figure 7: *Site 2, 120m segment of CCR data. A) CCR inverted resistivity section to depth of ~2.5m, RMS = 4.84%; B) CCR interpreted inverted section.*

DISCUSSION – *Karst Phenomena*

The Gypsum Plain of the Delaware Basin encompasses outcrop of strata that are dominantly composed of gypsum or anhydrite of the Castile Formation (Olive, 1957). Karst development is the result of a complex interaction between surficial geomorphology, hydrogeologic regimes on a local and regional scale, and local variations in lithology (Stafford, 2008a). Evaporitic rocks possess high solubility, therefore have the potential to form dramatic karst landscapes through natural processes and intensified by anthropogenic modifications. Within the study area, suffosion karst have the highest geohazard potential and are likely connected to deeper karst features that allow sediment and fluid transport. Due to the low permeability of gypsum, heavy rain events dissolve the evaporite rocks primarily by widening solution fractures within gypsum bedrock. The solution fractures enable fluids to migrate through sulfate rocks promoting development of conduits and enabling greater piping rates of gypsite soil, that subsequently collapse.

Throughout the Gypsum Plain, zones of brecciation have been well-documented in the evaporite strata of the Castile, Salado and Rustler formations (Anderson & Kirkland, 1980). Breccia forms from intrastratal dissolution of evaporites through hypogene speleogenesis where ascending fluids create void space that is later collapsed. Calcitization is commonly found in

regions of brecciation where vertically and laterally extensive calcitized breccia zones have developed. The same transmissive and soluble zones that allow for hypogene dissolution and brecciation create preferential flow paths for ascending hydrocarbons, which serve as the energy source for sulphate reducing bacteria associated with evaporite calcitization. Study Site 1 contains signature anomalies of a breccia pipe containing both brecciated gypsum and "plume-like" structures of calcitized gypsum associated with rising hydrocarbons.

The inverted resistivity sections observed from the CCR surveys collected at Site 2 revealed the presence of significant karst geohazards. This site shows a much thicker gypsite soil horizon in the resistivity profile section with a distinct contact with gypsum bedrock. Suffosion processes are interpreted to be the cause of both the observed fractures and the gypsite cave where soil has likely piped into the open gypsum cavities at depth.

Remote sensing data provided by TxDOT (orthoimagery and LiDAR data) and surficial geohazard mapping conducted in the summer of 2019 assisted with the interpretations. The range of resistivity anomalies observed in the selected study sites correlated well with surface manifestations of karst geohazards, but also include features that are not observed at the land surface.

CONCLUSION

The numerous expressions of evaporite karst found within the Gypsum Plain of the Delaware Basin can be observed in resistivity imaging, as well as exposed at the land surface throughout the outcrop region of the Castile and Rustler formations. The intensification in hydrocarbon extraction and exploration has led to an increase in development of vehicle infrastructure along with an associated rise of incidents related to karst geohazards. A critical element for improved infrastructure design and geohazard mitigation is the high-resolution characterization of potential geohazards that do not manifest at the land surface.

The study presented in this paper focused on a 30-mile (48 km) segment of undeveloped FM 2185 that traverses northward across the Gypsum Plain in Culberson County, Texas. Prior land reconnaissance surveys conducted during the summer of 2019 documented numerous surficial karst manifestations, including sinkholes, subsidence features, and caves. The full

length of the study area was initially surveyed utilizing CCR methods to rapidly delineate karst features that do not manifest at the land surface to depths up to ~2.5-meters.

The non-invasive geophysical method employed in this study quickly detected potential karst geohazards, but for proper characterization a combination of field mapping and excavation is required. Utilizing rapid CCR techniques can prove essential for geohazard mitigation and the improvement of vehicle infrastructure design to properly handle the weight and volume of oilfield traffic.

REFERENCES

AGI, 2007, Instruction Manual for EarthImager 2D Resistivity and IP Inversion Software: Austin, TX, Advanced Geosciences, Inc., 139pp.

Anderson, R.Y., and Kirkland, D.W., 1980, Dissolution of salt deposits by brine density flow. Geology, **8:** 66-69.

Barker, C.E., and Halley, R.B., 1986, Fluid inclusion, stable isotope, and vitrinite reflectance evidence for the thermal history of the Bone Spring Limestone, southern Guadalupe Mountains, Texas; *in* Gautier, D.L. (ed.), Roles of organic matter in sediment diagenesis: Soc. Econ. Paleontol. Mineral., Publ. 38, pp. 189-203.

Barker, C.E., and Pawlewicz, M.J., 1987, The effects of igneous intrusions and higher heat flow on thermal maturity of Leonardian and younger rocks, western Delaware Basin, Texas; *in* Cromwell, D.W. and Mazzullo, L. (eds.), Glass Mountains: Soc. Econ. Paleontol. Mineral., Guidebook, pp. 69-83.

Barker, C.E., and Pawlewicz, M.J., 1993, Post-tectonic reheating of portions of the Permian Basin as expressed by iso-reflectance lines on regional structural sections; *in* Love, D.W., et al. (eds.), Carlsbad region, New Mexico and West Texas: New Mexico Geol. Soc., Guidebook, 44th Ann. Field Conf., pp.29-30.

Ehrhart, J.T., 2016, Speleogenesis and Delineation of Megaporosity and Karst Geohazards Through Geologic Cave Mapping and LiDAR Analyses Associated with Infrastructure in Culberson County, Texas. Electronic Theses and Dissertations, Stephen F. Austin State University, 66.

EIA, 2020, Permian Basin, Part 1: Wolfcamp, Bone Spring, Delaware Shale Plays of the Delaware Basin: Washington, D.C., U.S. Department of Energy, 40 pp.

Hill, C. A., 1996, Geology of the Delaware Basin, Guadalupe, Apache and Glass Mountains: New Mexico and West Texas. Permian Basin Section – SEPM, Midland, Texas, 480 p.

Horak, R.L., 1985b, Trans-Pecos tectonism and its effects on the Permian Basin; *in* Dickerson, P.W. and Muehlberger, W.R. (eds.), Structure and tectonics of Trans-Pecos, Texas: West Texas Geol. Soc., Guidebook Publ. 85-81, Marine Minerals, Short Course, pp.81-87.

Keller, G.R., Hills, J.M., and Djeddi, R., 1980, A regional geological and geophysical study of the Delaware Basin, New Mexico and West Texas; *in* Dickerson, P.W. and Hoffer, J.M. (eds.), Trans-Pecos Region: New Mexico Geol. Soc., Guidebook, 31st Field Conf., pp. 105-111.

Klimchouk, A. B., and Aksem, S.D., 2005, Hydrochemistry and solution rates in gypsum karst: Case study from the Western Ukraine. Environmental Geology, vol. 48, no. 3, pp. 307-319. DOI: 10.1007/s00254-005-1277-3.

Land, L., Cikoski, C., McCraw, D., and Veni, G., 2018. Karst Geohazards and Geophysical Surveys: US 285, Eddy County, New Mexico, Report of Investigation 7. Carlsbad: National Cave and Karst Research Institute.

Lee, M.K. & Williams, D.D., 2000. *Paleohydrology of the Delaware Basin, western Texas: overpressure development, hydrocarbon migration, and ore genesis.* Bulletin of the American Association of Petroleum Geologists, v. 84, no .7, pp. 961-974.

Majzoub, A. F., Stafford, K. W., Brown, W. A., and Ehrhart, J. T., 2017, Characterization and Delineation of Gypsum Karst Geohazards Using 2D Electrical Resistivity Tomography in Culberson County, Texas, USA. Journal of Environmental and Engineering Geophysics, vol 22, no. 4, pp.411-420.

Neukum, C., Grutzner, C., Azzam, R., and Reicherter, K., 2010, Mapping buried karst features with capacitive-coupled resistivity system (CCR) and ground penetrating radar (GPR). Advances in Research in Karst Media (2010): p. 429-434.

Olive, W.W., 1957, Solution-subsidence troughs, Castile Formation of Gypsum Plain, Texas and New Mexico: GSA Bull., v. 68, no. 3, pp. 351-358.

Scholle, P.A., Goldstein, R.H., and Ulmer-Scholle, D.S., 2004, Classic Upper Paleozoic Reefs and Bioherms of West Texas and New Mexico. New Mexico Institute of Mining and Technology, Socorro, NM, 166p.

Stafford, K., Brown, W., Ehrhart, J., Majzoub, A., and Woodard, J., 2017, Evaporite karst geohazards in the Delaware Basin, Texas: Review of traditional karst studies coupled with geophysical and remote sensing characterization. International Journal of Speleology, 46, 169-180.

Stafford, K., Ehrhart, J., Majzoub, A., Shields, J., and Brown, W., 2018. Unconfined hypogene evaporite karst: west Texas and southeastern New Mexico, USA: International Journal of Speleology 47-3, 293-305.

Stafford, K.W., Nance, R., Rosales-Lagarde, L., and Boston, P.J., 2008a, Epigene and hypogene karst manifestations of the Castile Formation: Eddy County, New Mexico and Culberson County, Texas. International Journal of Speleology, v. 37, no.2, pp. 83-98.

Stafford, K.W., Rosales-Lagarde, L., and Boston, P.J., 2008b, Castile evaporite karst potential map of the Gypsum Plain, Eddy County, New Mexico and Culberson County, Texas: A GIS methodological comparison. Journal of Cave and Karst Studies, vol. 70, no. 1, pp. 35-46.

Stafford, K.W., Ulmer-Scholle, D., and Rosales-Lagarde, L., 2008c, Hypogene calictization: Evaporite diagenesis in the western Delaware Basin: Carbonates and Evaporites, v. 23, pp. 89-103.

Woodard, J.D., 2017, “Geophysical Delineation of Megaporosity and Fluid Migration Pathways for Geohazard Characterization within the Delaware Basin, Culberson County, Texas”. Electronic Theses and Dissertations. 137. https://scholarworks.sfasu.edu/etds/137